

# Variable absorption of mutational trends by prion-forming domains during *Saccharomyces* evolution

Paul M Harrison <sup>Corresp. 1</sup>

<sup>1</sup> Dept. of Biology, McGill University, Montréal, Quebec, Canada

Corresponding Author: Paul M Harrison  
Email address: paul.harrison@mcgill.ca

Prions are self-propagating alternative states of protein domains. They are linked to both diseases and functional protein roles in eukaryotes. Prion-forming domains in *Saccharomyces cerevisiae* are typically domains with high intrinsic protein disorder (*i.e.*, that remain unfolded in the cell most of the time), that are converted to self-replicating amyloid forms. It is still unclear what principles might govern the molecular evolution of prion-forming domains, and intrinsically disordered domains generally. Here, it is discovered that in a set of such prion-forming domains some evolve in the fungal class *Saccharomyces* in such a way as to absorb general mutation biases across millions of years, whereas others do not, indicating a spectrum of selection pressures on composition and sequence. Thus, if the bias-absorbing prion formers are conserving a prion-forming capability, then this capability is not interfered with by the absorption of bias changes over vast evolutionary epochs. These results suggest methodology for assessing selection pressures on the composition of intrinsically disordered regions.

1

2 **Variable absorption of mutational trends by prion-forming domains**  
3 **during *Saccharomyces* evolution**

4

5

6 Department of Biology,

7 McGill University,

8 Montreal, QC,

9 Canada.

10

11 Corresponding author:

12 Paul Harrison

13 Email: [paul.harrison@mcgill.ca](mailto:paul.harrison@mcgill.ca)

14

15

16

## 17 **Abstract:**

18 Prions are self-propagating alternative states of protein domains. They are linked to both  
19 diseases and functional protein roles in eukaryotes. Prion-forming domains in *Saccharomyces*  
20 *cerevisiae* are typically domains with high intrinsic protein disorder (*i.e.*, that remain unfolded in  
21 the cell most of the time), that are converted to self-replicating amyloid forms. It is still unclear  
22 what principles might govern the molecular evolution of prion-forming domains, and intrinsically  
23 disordered domains generally. Here, it is discovered that in a set of such prion-forming domains  
24 some evolve in the fungal class *Saccharomycetes* in such a way as to absorb general mutation  
25 biases across millions of years, whereas others do not, indicating a spectrum of selection pressures  
26 on composition and sequence. Thus, if the bias-absorbing prion formers are conserving a prion-  
27 forming capability, then this capability is not interfered with by the absorption of bias changes  
28 over vast evolutionary epochs. These results suggest methodology for assessing selection pressures  
29 on the composition of intrinsically disordered regions.

30

## 31 **Introduction**

32 Prion formation and propagation have been studied extensively in the budding yeast  
33 *Saccharomyces cerevisiae*. The yeast *S. cerevisiae* has >200 prion-like proteins that have N/Q-rich  
34 domains of the sort observed in  $\geq 8$  known prion-formers (An et al. 2016). Such yeast prions have  
35 been linked to diverse phenomena including evolutionary capacitance, disease-like states, and  
36 large-scale genetic control. The first well-characterized yeast prions, that underlie the [PSI<sup>+</sup>] and  
37 [URE3] prions, are propagating amyloids of the proteins Sup35p and Ure2p respectively. The  
38 protein Sup35p is part of the translation termination complex. [PSI<sup>+</sup>] prion formation reduces  
39 translation termination efficiency and increases nonsense-codon read-through levels (Cox 1965;

40 Shorter & Lindquist 2005). This read-through has been shown to have a potential role in  
41 uncovering cryptic genetic variation (True et al. 2004; True & Lindquist 2000). [URE3] causes  
42 upregulation of poor nitrogen source usage, even when rich sources are available (Lacroute 1971;  
43 Wickner 1994; Wickner et al. 2004). Prion variants sometimes behave as budding-yeast diseases  
44 (McGlinchey et al. 2011; Nakayashiki et al. 2005). The [MOT3+] prion has been shown to have a  
45 possible role in control of transitions to multicellularity (Holmes et al. 2013). The stress-inducible  
46 cytoskeleton-linked budding-yeast protein Lsb2 (also known as Pin3) can form a metastable prion  
47 in response to high temperatures (Chernova et al. 2017a; Chernova et al. 2017b). There are now  
48 several known amyloid-based prions of *S. cerevisiae* (Harbi & Harrison 2014a; Harbi et al. 2012).  
49 Prion-forming proteins have also been discovered in the fungus *Podospora anserina* and the  
50 fission yeast *Schizosaccharomyces pombe* (Saupe 2011; Sideri et al. 2017). Amyloid-based  
51 budding yeast prion-forming regions tend to have high intrinsic disorder and a bias for asparagine  
52 (N) and/or glutamine (Q) residues (Harbi & Harrison 2014b). Several algorithms have been  
53 developed that annotate protein regions with high potential prion-forming propensity (Espinosa  
54 Angarica et al. 2013; Lancaster et al. 2014; Ross et al. 2013; Zambrano et al. 2015). Prion-like  
55 proteins in yeast and other organisms have more recently been linked to other processes, such as  
56 the formation of stress granules and other membraneless biomolecular condensates (Franzmann et  
57 al. 2018; Jain et al. 2016).

58         The original mammalian PrP domain is not biased for Ns and Qs, and is deeply conserved  
59 since a PrP ancestral gene emerged in early chordate evolution, likely through retrotransposition  
60 (Ehsani et al. 2011; Harrison et al. 2010; Westaway et al. 2011). The [PSI+] prion has an N/Q bias  
61 that is conserved across *Ascomycota* and *Basidiomycota*, which diverged >1 billion years ago  
62 (Harrison et al. 2007). A large population of yeast-prion-like proteins emerged *en masse* early in

63 *Saccharomyces* evolution, as a result of mutational trends to form more polyasparagine runs,  
64 thus providing an evolutionary ‘test set’ from which several prion-forming domains seem to have  
65 developed (An et al. 2016). Prion-forming domains from *S. cerevisiae* tend to evolve more  
66 quickly as sequences than other prion-like domains but maintain their prion-like composition (Su  
67 & Harrison 2019). Eukaryotes often bear large numbers of these prion-like domains in their  
68 proteins. The slime mold *Dictyostelium* has >20% prion-like proteins (An & Harrison 2016;  
69 Malinovska et al. 2015), and there is evidence it has evolved a system to subvert prion formation  
70 (Malinovska & Alberti 2015; Malinovska et al. 2015). Other organisms such as *Drosophila*  
71 *melanogaster*, *Plasmodium falciparum* and the leech *Helobdella robusta* have high percentages of  
72 prion-like proteins in their proteomes (An & Harrison 2016; Pallares et al. 2018). In humans,  
73 several other yeast-prion-like proteins have links to neurodegeneration (Kim et al. 2013;  
74 Pokrishevsky et al. 2016; Sun et al. 2011). In *Aplysia* and *Drosophila*, such proteins have been  
75 linked to long-term memory formation (Khan et al. 2015; Si et al. 2010). Predicted prions can be  
76 observed in all the domains of life (Espinosa Angarica et al. 2013), including thousands in  
77 viruses and phages (Tetz & Tetz 2017; Tetz & Tetz 2018), and tens of thousands in bacteria  
78 (Harrison 2019; Iglesias et al. 2015). Bacterial prion-forming proteins have been detected  
79 experimentally (Molina-Garcia et al. 2018; Shahnawaz et al. 2017; Yuan et al. 2014; Yuan &  
80 Hochschild 2017). Bacterial prion-like proteins have a characteristic pattern of evolutionarily  
81 ancient, multi-phylum distribution coupled to sparse, intermittent conservation across their  
82 evolutionary range of species (Harrison 2019). About 5% of compositionally-biased dark matter  
83 (*i.e.*, regions that cannot be assigned as either structured or intrinsically disordered) in the known  
84 protein universe are predicted to be prion-like domains (Harrison 2018).

85 Here, the evolution of the sequences of prion-forming domains in *Saccharomyces* is re-  
86 visited, but from the point of view of mutation biases. It is discovered that these protein regions  
87 have a spectrum of behaviour, variably absorbing mutation biases that are observable in the  
88 proteome as a whole, evidenced in the numbers of prion-like proteins, the % guanidine and cytidine  
89 (GC%) in the DNA, and the proportions of poly-asparagine and poly-glutamine.

90

## 91 **Methods**

### 92 *Data*

93 The UniProt (Boeckmann et al. 2003) set of reference fungal proteomes for  
94 *Saccharomyces* (73 organisms) was downloaded from [www.uniprot.org](http://www.uniprot.org) in June 2017. Sets of  
95 proteins with prion-forming domains (Data S1) and their orthologs across *Saccharomyces* were  
96 collated as previously described (Su & Harrison 2019).

97

### 98 *Prion-like composition*

99 Prion-like composition in orthologs was calculated in two ways, firstly using the PLAAC  
100 prion-like domain annotation program (Lancaster et al. 2014), and secondly using the fLPS  
101 program for annotation of compositional biases (Harrison 2017). These were both run using default  
102 parameters, except that for fLPS the expected frequency for glutamine and asparagine residues  
103 was set equal to 0.05. For PLAAC, both the PRD score and the LLR score were analysed; the  
104 former is an indicator of the overall amount of prion-like composition in an annotated bounded  
105 prion-like region, while the latter indicates the prion-like sequence composition of the best  
106 sequence window (Lancaster et al. 2014). Any PLAAC score values that are negative or 'N/A' in  
107 the output from PLAAC are set equal to 0.0 for the purposes of this analysis.

108

109 ***Measures of proteome bias***

110 Several measures of compositional bias across proteomes/genomes were examined:

111 (i) %N (asparagine) in the proteome;

112 (ii) %Q (glutamine) in the proteome;

113 (iii) % poly-N in the proteome (with a minimum tract length of 3);

114 (iv) % poly-Q in the proteome (with a minimum tract length of 3);

115 (v) % poly-Q + poly-N in the proteome (with a minimum tract length of 3);

116 (vi) %GC in the DNA;

117 (vii) The fraction of N/Q-rich proteins in the proteome according to a specific fLPS bias P-  
118 value threshold (either 1e-08, 1e-10 or 1e-12);

119 (viii) The fraction of proteins in the proteome with prion-like composition according to the  
120 program PLAAC (with PRD score >0.0,  $\geq 15.0$  or  $\geq 30.0$ , or similarly for LLR score).

121

122 ***Correlations***

123 Both weighted and unweighted Pearson correlation coefficients were calculated to assess  
124 the correlations of individual prion-like composition with the general trends in the proteome.

125 Weightings for plot points were calculated according to their closest similarity with another  
126 protein, calculated as  $(1 - \%I/100)$ , where %I is the percentage sequence identity in the most

127 significant BLASTP sequence alignment (Altschul et al. 1997). These weightings were summed

128 appropriately, as described in previous analyses (Harrison 2019; Su & Harrison 2019). Results

129 indicate that the overall outcomes for specific proteins are not affected by non-usage of such

130 weightings (see below).

131

## 132 **Results**

### 133 *Ure2 protein*

134 As an initial example, the evolutionary behaviour of compositional biases in the prion-  
135 forming domain of Ure2p was examined (Figures 1-2). The current data indicate that an ancestor  
136 of the Ure2p prion-forming domain with a strong N/Q-rich prion-like composition originated early  
137 in *Saccharomyces* evolution (at least in the last common ancestor of the diverse families  
138 *Debaryomycetaceae* and *Saccharomycetaceae*), in agreement with results in previous publications  
139 (An et al. 2016; Harrison et al. 2007) (Figure 3). In general, there is a strong correlation between  
140 the degree of bias in the N/Q-rich region of Ure2p and the degree of compositional bias in the  
141 whole proteome/genome by several indicators (%polyasparagine or  
142 %[polyasparagine+polyglutamine] or DNA GC% or fraction of N/Q-rich prion-like proteins with  
143 fLPS P-value  $<10^{-10}$ ) (Figure 1). The correlations with PLAAC prion-like composition score are  
144 lower, but both measures have strong correlations with %GC in DNA (Figure 2). Thus, during the  
145 surge in formation of prion-like regions during *Saccharomyces* evolution (An et al. 2016), the  
146 degree of N-bias in the individual prion-former Ure2p also increased in correlation with the general  
147 trend as it panned out across various sub-clades.

148

### 149 *Other prion-forming proteins*

150 Of the known amyloid-based prions—as well as Ure2p—Swi1p, Cyc8p and Sup35p have  
151 domains of prion-like composition or N/Q bias that are widespread across *Saccharomyces* (in  
152 84% of orthologs for Cyc8p, 98% for Swi1p, and 90% for Sup35p; Table S1), with such domains  
153 of these latter three also arising in other *Ascomycota* clades (An et al. 2016; Harrison et al. 2007).

154 Furthermore, Pin3 protein also has a widespread prion-like domain across *Saccharomyces*, there  
155 being 52/55 (95%) *Saccharomyces* Pin3 orthologs having PLAAC LLR scores >15.0. However,  
156 the degree of conservation of N/Q-rich bias *per se* is lower for this protein with 38/55 (75%) having  
157 a fLPS compositional bias P-value  $\leq 1e-10$ . The metastable prion domain of Pin3 is the only known  
158 amyloid-based prion in *S. cerevisiae* to demonstrate very little correlation for its prion-like  
159 compositional biases, indicating some selection pressure for composition of a different sort, that  
160 nonetheless may preserve prion-forming ability.

161         The other three cases (Mot3p, Rnq1p and Nu100p) have either more recent ancestry as  
162 novel prion-like domains within *Saccharomyces* (in the case of Mot3p and Rnq1p), or they arise  
163 sporadically in fungal species (Nu100p) (An et al. 2016; Su & Harrison 2019). These three are  
164 thus not expected to demonstrate many significant correlations with measures of compositional  
165 bias, but nonetheless we see a mild negative correlation for Rnq1p and Mot3p with %Q in the  
166 proteome, which is not typical of the other prion-forming proteins, suggesting selection pressures  
167 against Q bias in these evolutionarily recently emergent proteins.

168         In general, there are strong correlations for Ure2p, Swip and Cyc8p with %N, %poly-N,  
169 %GC in DNA and with the numbers of proteins with prion-like composition (Tables 4-5). Within  
170 these general trends, these four demonstrate a spectrum of responses to the overall proteome-wide  
171 mutational trends, with Ure2p being the strongest correlator. Sup35p stands out as an exception; it  
172 shows on the whole weaker correlations generally with %N and %poly-N, and stronger  
173 correlations with %poly-Q than the other three. This may be because there is selection pressure to  
174 maintain a specific proportion of Qs in specific local patterns or ratios (MacLea et al. 2015).

175         There is one species that is often a far outlier on the plots, *Ascoidea rubescens*, an  
176 uncharacterized species that is the sole member of the family *Ascoideaceae*, which is

177 geographically widely distributed and typically grows in beetle galleries in dead wood. It has a  
178 very high proportion of poly-N-rich proteins (Tables 1-2). Removal of this outlier species from  
179 the correlation analysis causes a substantial increase in correlations with %N and %poly-N, but  
180 not for %GC in DNA.

181 Thus, the three *S. cerevisiae* prion-forming proteomes Ure2p, Cyc8p and Swi1p appear to  
182 absorb the general mutational trends linked to the surge in formation of prion-like domains, that  
183 was observed previously (An et al. 2016). This trend is linked to a general decrease in %GC in the  
184 DNA (Tables 1-2).

185 Two other separately studied prion-forming domains are from New1p and Pub1p (Li et al.  
186 2014; Osherovich & Weissman 2001). These are both strongly correlated proteome-bias absorbers,  
187 with Pub1p (which is an interaction hub for other prion-like proteins (Harbi & Harrison 2014b))  
188 uniquely amongst all of the prion-forming domains displaying a strong correlation for both poly-  
189 N and poly-Q (Tables 1-2). Pub1p is strongly correlated despite having a low number of  
190 orthologous prion domains that have high bias for N and Q residues (53% with fLPS P-value  $\leq 1e-$   
191 10; Table S1) indicating that there is still correlated behavior for the weaker N/Q biases for this  
192 protein. Other prion-forming domains observed in the analysis of Alberti, *et al.* (Alberti et al.  
193 2009), also display a similar spectrum of bias absorption across *Saccharomyces* evolution (Table  
194 S2). Highly-correlated bias absorbers from this data whose prion-like domains are widespread in  
195 *Saccharomyces* include Lsm4p and Gln3p, whereas other widespread prion-like domains show  
196 little or no correlation, such as Ngr1p (Tables S1, S2).

197 The above analysis uses the PLAAC PRDscore, to define the amount of prion-like  
198 composition in a bounded region, and so reflecting more absorption of biases in a way analogous  
199 to the working of the fLPS algorithm (Harrison 2017; Lancaster et al. 2014). The PLAAC log-

200 likelihood ratio (LLR) score has been used in the literature to pick out the most likely prion-  
201 forming sequence window within proteins (Alberti et al. 2009; An et al. 2016; Sideri et al. 2017;  
202 Tetz & Tetz 2018). Despite the restriction of a window of fixed size (41 amino-acid residues),  
203 these LLR scores also demonstrate a similar spectrum of bias absorption, with both strong and  
204 weak absorbers evident, albeit generally with less significance (Table S3).

205         It was checked whether the N/Q-rich regions are also rich in lysine, which is encoded by  
206 AT%-rich codons, like N (asparagine). Lysine has low prion formation propensity and charged  
207 residues are disruptive to prion formation and have low prion formation propensity (Lancaster et  
208 al. 2014; Osherovich & Weissman 2001). Lysine is a disorder-promoting residue (Oldfield &  
209 Dunker 2014) and some intrinsically disordered regions have high positive charge (Hatos et al.  
210 2020; Necci et al. 2018). However, the N/Q-rich regions consistently in general have lower lysine  
211 content than the whole *Saccharomyces* proteomes (Figure 4). Thus, these regions are not simply  
212 absorbing higher levels of AT% in their DNA through the embedding within them of amino-acid  
213 residues encoded by codons with high AT%.

214

## 215 **Discussion**

216         These results indicate that compositional aspects of many individual prion-formers  
217 behaved in a correlated way in relation to general trends as they panned out over millions of years  
218 across various sub-clades. Also, this surge in prion-like region formation is directly linked to a  
219 general trend for GC% decrease across the *Saccharomyces* clade. However, some prion-forming  
220 domains resist the absorption of such mutational trends, such as the meta-stable prion-former  
221 Lsb2/Pin3 (Chernova et al. 2017b), despite it being as widely conserved as a protein as those that  
222 more easily absorb biases, such as Cyc8p and Swi1p. This suggests some greater selection pressure

223 on amino-acid composition. The Sup35p prion-forming domain also shows some special behavior:  
224 demonstrating a stronger correlation between overall proteome poly-Q levels and its own N or Q  
225 compositional bias as determined by the program fLPS. The Sup35 prion-forming domain has a  
226 subdomain with specific local patterns involving Q residues that is required for chaperone-  
227 dependent prion maintenance, that is separate from the N-terminal N/Q-rich region that is  
228 necessary for prion nucleation and fibre growth (MacLea et al. 2015). Also, the Sup35 prion-like  
229 domain has a more ancient origin before the last common ancestor of *Saccharomyces*, and  
230 outside this clade it tends to have a predominant Q-bias that has been maintained within  
231 *Saccharomyces*, resisting the trend for greater N-bias (An et al. 2016). However, this is also the  
232 behaviour of Cyc8p and Swi1p outside of *Saccharomyces* (An et al. 2016), so this result is  
233 demonstrating an evolutionary behavior peculiar to Sup35p.

234 The Pub1p prion-forming domain shows strong correlations for both Q and N bias  
235 indicators. It is possible that proteins such as Pub1p that interact a lot with other prion-like proteins  
236 (Harbi & Harrison 2014b) 'need' to absorb more general compositional trends so that they can  
237 promiscuously bind with a large list of partners.

238 The results here provide a case study of mutational trend absorption by disordered regions  
239 generally. The results suggest some methodology for analyzing selection pressures on individual  
240 intrinsically disordered regions within the context of the behaviour of other sequences within the  
241 same proteome.

242

## 243 **Conclusions**

244 Thus, many prion-forming domains, and intrinsically disordered regions generally, are  
245 continually absorbing overall mutational trends in their proteomes, but this is modulated by

246 specific selection pressures. A spectrum of bias absorption is observed from Lsb2/Pin3---which  
247 shows little or no correlation---to Pub1, which shows very strong correlation to both asparagine-  
248 and glutamine-based biases.

249

## 250 **Supplementary Materials**

251 **Data S1: FASTA-format file of the protein sequences of the proteins with prion-forming**  
252 **domains.**

253

254 **Table S1: Fraction of orthologs that have prion-like composition.**

255

256 **Table S2: Table of results for the other prion-forming proteins from ref. (Alberti et al. 2009).**

257

258 **Table S3: Correlations using PLAAC LLR score instead of PRD score.**

259

260

261

262 **Figure Legends**

263 **Figure 1: Correlation of various measures of mutational bias across proteomes versus the**  
264 **individual compositional bias in the Ure2p prion-forming domain, as judged by the fLPS**  
265 **program.**

- 266 (a) Percentage of poly-N residues in the proteome.  
267 (b) Percentage of (poly-N + poly-Q) residues in the proteome.  
268 (c) DNA GC%.  
269 (d) Fraction of N/Q-rich prion-like proteins with fLPS P-value  $<1e-10$ .  
270 (e) Table of correlations and significances for plots (a) to (d).

271

272 **Figure 2: As in Figure 1, except versus the individual PLAAC PRDscore in the Ure2p prion-**  
273 **forming domain.**

- 274 (a) Percentage of poly-N residues in the proteome.  
275 (b) Percentage of (poly-N + poly-Q) residues in the proteome.  
276 (c) DNA GC%.  
277 (d) Fraction of proteome with PLAAC score  $\geq 15.0$ .  
278 (e) Table of correlations and significances for plots (a) to (d).

279

280 **Figure 3: Schematic evolutionary tree showing the distribution of orthologs with prion-like**  
281 **composition in different evolutionary families in the Uniprot reference set of fungal**  
282 **proteomes (Boeckmann et al. 2003).** The organismal branching pattern from recent fungal  
283 phylogenies was used (Kurtzman & Robnett 2013; Shen et al. 2016). The number of species in

284 each family is given in brackets. The numbers of orthologs that are have fLPS P-value  $\leq 1e-10$  and  
285 PLAAC score  $\geq 15.0$  are listed in columns (Harrison 2017; Lancaster et al. 2014).

286

287 **Figure 4: Correlations of %K (lysine residues) within the N/Q-rich regions of prion-forming**  
288 **proteins plotted versus the overall %K trend in proteomes.** Blue points are for the set of known  
289 amyloid-based prions in Figure 4, and orange points for the total list of prion-forming domains  
290 including those listed in Table S2.

291

## 292 Table Legends

293 **Table 1: Coloured table for a set of known prion-forming domains of the correlations**  
294 **(weighted and un-weighted) between the compositional bias ( $-\log[\text{fLPS P-value}]$ ), and a**  
295 **variety of parameters.** Weighted correlations are the upper value in each cell, unweighted the  
296 lower value. Where removal of the common far outlier species *Ascoidea rubescens* causes  
297 increased significance for any correlation, the third and fourth rows in a cell display the correlation  
298 coefficients (in italics). For proteins which do not have an ortholog from *Ascoidea rubescens*, the  
299 name is labelled with ‘††’. If its removal causes no improvement in correlations, it is labelled with  
300 ‘†’. Correlations significant at  $\leq 0.0005$  are labelled \*\*\* and coloured green, significant at  $> 0.0005$   
301 and  $\leq 0.0016$  labelled \*\* and coloured orange, and  $> 0.0016$ , and  $\leq 0.05$  are labelled \*). The  
302 threshold 0.0016 comes from a Bonferroni correction to allow for the fact that 31 sequences are  
303 being tested for a correlation against any specific proteome-wide property. In column one, the  
304 name is colour-coded according to the most significant correlation, with underlining if it is a 1-\*  
305 correlation.

306

307 **Table 2: Coloured table for a set of known prion-forming domains of the correlations (both**  
308 **weighted and un-weighted) between the prion-like composition (PLAAC PRDscore) and a**  
309 **variety of parameters.** Weighted correlations are the upper value in each cell, unweighted the  
310 lower value. Where removal of the common far outlier species *Ascoidea rubescens* causes  
311 increased significance for any correlation, the third and fourth rows in a cell display the correlation  
312 coefficients (in italics). For proteins which do not have an ortholog from *Ascoidea rubescens*, the  
313 name is labelled with ‘††’. If its removal causes no improvement in correlations, it is labelled with  
314 ‘†’. Correlations significant at  $\leq 0.0005$  are labelled \*\*\* and coloured green, significant at  $> 0.0005$   
315 and  $\leq 0.0016$  labelled \*\* and coloured orange, and  $> 0.0016$ , and  $\leq 0.05$  are labelled \*). The  
316 threshold 0.0016 comes from a Bonferroni correction to allow for the fact that 31 sequences are  
317 being tested for a correlation against any specific proteome-wide property. In column one, the  
318 name is colour-coded according to the most significant correlation, with underlining if it is a 1-\*  
319 correlation.

320

321

## 322 **References**

323 Alberti S, Halfmann R, King O, Kapila A, and Lindquist S. 2009. A systematic survey identifies  
324 prions and illuminates sequence features of prionogenic proteins. *Cell* 137:146-158.

325 Altschul SF, Madden TL, Schaffer AA, Zhang J, Zhang Z, Miller W, and Lipman DJ. 1997.

326 Gapped BLAST and PSI-BLAST: a new generation of protein database search programs.

327 *Nucleic Acids Res* 25:3389-3402.

328 An L, Fitzpatrick D, and Harrison PM. 2016. Emergence and evolution of yeast prion and prion-

329 like proteins. *BMC Evol Biol* 16:24. 10.1186/s12862-016-0594-3

- 330 An L, and Harrison PM. 2016. The evolutionary scope and neurological disease linkage of yeast-  
331 prion-like proteins in humans. *Biol Direct* 11:32. 10.1186/s13062-016-0134-5
- 332 Boeckmann B, Bairoch A, Apweiler R, Blatter MC, Estreicher A, Gasteiger E, Martin MJ,  
333 Michoud K, O'Donovan C, Phan I, Pilbout S, and Schneider M. 2003. The SWISS-PROT  
334 protein knowledgebase and its supplement TrEMBL in 2003. *Nucleic Acids Res* 31:365-  
335 370.
- 336 Chernova TA, Chernoff YO, and Wilkinson KD. 2017a. Prion-based memory of heat stress in  
337 yeast. *Prion* 11:151-161. 10.1080/19336896.2017.1328342
- 338 Chernova TA, Kiktev DA, Romanyuk AV, Shanks JR, Laur O, Ali M, Ghosh A, Kim D, Yang  
339 Z, Mang M, Chernoff YO, and Wilkinson KD. 2017b. Yeast Short-Lived Actin-  
340 Associated Protein Forms a Metastable Prion in Response to Thermal Stress. *Cell Rep*  
341 18:751-761. 10.1016/j.celrep.2016.12.082
- 342 Cox B. 1965. [PSI], a cytoplasmic suppressor of super-suppression in yeast. *Heredity* 20:505-  
343 521.
- 344 Ehsani S, Tao R, Pocanschi CL, Ren H, Harrison PM, and Schmitt-Ulms G. 2011. Evidence for  
345 retrogene origins of the prion gene family. *PLoS One* 6:e26800.  
346 10.1371/journal.pone.0026800
- 347 Espinosa Angarica V, Ventura S, and Sancho J. 2013. Discovering putative prion sequences in  
348 complete proteomes using probabilistic representations of Q/N-rich domains. *BMC*  
349 *Genomics* 14:316. 10.1186/1471-2164-14-316
- 350 Franzmann TM, Jahnel M, Pozniakovsky A, Mahamid J, Holehouse AS, Nuske E, Richter D,  
351 Baumeister W, Grill SW, Pappu RV, Hyman AA, and Alberti S. 2018. Phase separation  
352 of a yeast prion protein promotes cellular fitness. *Science* 359. 10.1126/science.aao5654

- 353 Harbi D, and Harrison PM. 2014a. Classifying prion and prion-like phenomena. *Prion* 8.
- 354 Harbi D, and Harrison PM. 2014b. Interaction networks of prion, prionogenic and prion-like  
355 proteins in budding yeast, and their role in gene regulation. *PLoS One* 9:e100615.  
356 10.1371/journal.pone.0100615
- 357 Harbi D, Parthiban M, Gendoo DM, Ehsani S, Kumar M, Schmitt-Ulms G, Sowdhamini R, and  
358 Harrison PM. 2012. PrionHome: a database of prions and other sequences relevant to  
359 prion phenomena. *PLoS One* 7:e31785.
- 360 Harrison LB, Yu Z, Stajich JE, Dietrich FS, and Harrison PM. 2007. Evolution of budding yeast  
361 prion-determinant sequences across diverse fungi. *J Mol Biol* 368:273-282.
- 362 Harrison PM. 2017. fLPS: Fast discovery of compositional biases for the protein universe. *BMC*  
363 *Bioinformatics* 18:476. 10.1186/s12859-017-1906-3
- 364 Harrison PM. 2018. Compositionally biased dark matter in the protein universe.  
365 *Proteomics*:e1800069. 10.1002/pmic.201800069
- 366 Harrison PM. 2019. Evolutionary behaviour of bacterial prion-like proteins. *PLoS One*  
367 14:e0213030. 10.1371/journal.pone.0213030
- 368 Harrison PM, Khachane A, and Kumar M. 2010. Genomic assessment of the evolution of the  
369 prion protein gene family in vertebrates. *Genomics* 95:268-277.  
370 10.1016/j.ygeno.2010.02.008
- 371 Hatos A, Hajdu-Soltesz B, Monzon AM, Palopoli N, Alvarez L, Aykac-Fas B, Bassot C, Benitez  
372 GI, Bevilacqua M, Chasapi A, Chemes L, Davey NE, Davidovic R, Dunker AK, Elofsson  
373 A, Gobeill J, Foutel NSG, Sudha G, Guharoy M, Horvath T, Iglesias V, Kajava AV,  
374 Kovacs OP, Lamb J, Lambrugh M, Lazar T, Leclercq JY, Leonardi E, Macedo-Ribeiro  
375 S, Macossay-Castillo M, Maiani E, Manso JA, Marino-Buslje C, Martinez-Perez E,

376 Meszaros B, Micetic I, Minervini G, Murvai N, Necci M, Ouzounis CA, Pajkos M,  
377 Paladin L, Pancsa R, Papaleo E, Parisi G, Pasche E, Barbosa Pereira PJ, Promponas VJ,  
378 Pujols J, Quaglia F, Ruch P, Salvatore M, Schad E, Szabo B, Szaniszlo T, Tamana S,  
379 Tantos A, Veljkovic N, Ventura S, Vranken W, Dosztanyi Z, Tompa P, Tosatto SCE, and  
380 Piovesan D. 2020. DisProt: intrinsic protein disorder annotation in 2020. *Nucleic Acids*  
381 *Res* 48:D269-D276. 10.1093/nar/gkz975

382 Holmes DL, Lancaster AK, Lindquist S, and Halfmann R. 2013. Heritable remodeling of yeast  
383 multicellularity by an environmentally responsive prion. *Cell* 153:153-165.

384 Iglesias V, de Groot NS, and Ventura S. 2015. Computational analysis of candidate prion-like  
385 proteins in bacteria and their role. *Front Microbiol* 6:1123. 10.3389/fmicb.2015.01123

386 Jain S, Wheeler JR, Walters RW, Agrawal A, Barsic A, and Parker R. 2016. ATPase-Modulated  
387 Stress Granules Contain a Diverse Proteome and Substructure. *Cell* 164:487-498.  
388 10.1016/j.cell.2015.12.038

389 Khan MR, Li L, Perez-Sanchez C, Saraf A, Florens L, Slaughter BD, Unruh JR, and Si K. 2015.  
390 Amyloidogenic Oligomerization Transforms Drosophila Orb2 from a Translation  
391 Repressor to an Activator. *Cell* 163:1468-1483. 10.1016/j.cell.2015.11.020

392 Kim HJ, Kim NC, Wang YD, Scarborough EA, Moore J, Diaz Z, MacLea KS, Freibaum B, Li S,  
393 Molliex A, Kanagaraj AP, Carter R, Boylan KB, Wojtas AM, Rademakers R, Pinkus JL,  
394 Greenberg SA, Trojanowski JQ, Traynor BJ, Smith BN, Topp S, Gkazi AS, Miller J,  
395 Shaw CE, Kottlors M, Kirschner J, Pestronk A, Li YR, Ford AF, Gitler AD, Benatar M,  
396 King OD, Kimonis VE, Ross ED, Wehl CC, Shorter J, and Taylor JP. 2013. Mutations in  
397 prion-like domains in hnRNPA2B1 and hnRNPA1 cause multisystem proteinopathy and  
398 ALS. *Nature* 495:467-473. 10.1038/nature11922

- 399 Kurtzman CP, and Robnett CJ. 2013. Relationships among genera of the Saccharomycotina  
400 (Ascomycota) from multigene phylogenetic analysis of type species. *FEMS Yeast Res*  
401 13:23-33. 10.1111/1567-1364.12006
- 402 Lacroute F. 1971. Non-Mendelian mutation allowing ureidosuccinic acid uptake in yeast. *J*  
403 *Bacteriol* 106:519-522.
- 404 Lancaster AK, Nutter-Upham A, Lindquist S, and King OD. 2014. PLAAC: a web and  
405 command-line application to identify proteins with prion-like amino acid composition.  
406 *Bioinformatics* 30:2501-2502. 10.1093/bioinformatics/btu310
- 407 Li X, Rayman JB, Kandel ER, and Derkatch IL. 2014. Functional role of Tia1/Pub1 and Sup35  
408 prion domains: directing protein synthesis machinery to the tubulin cytoskeleton. *Mol*  
409 *Cell* 55:305-318. 10.1016/j.molcel.2014.05.027
- 410 MacLea KS, Paul KR, Ben-Musa Z, Waechter A, Shattuck JE, Gruca M, and Ross ED. 2015.  
411 Distinct amino acid compositional requirements for formation and maintenance of the  
412 [PSI(+)] prion in yeast. *Mol Cell Biol* 35:899-911. 10.1128/MCB.01020-14
- 413 Malinowska L, and Alberti S. 2015. Protein misfolding in Dictyostelium: Using a freak of nature  
414 to gain insight into a universal problem. *Prion* 9:339-346.  
415 10.1080/19336896.2015.1099799
- 416 Malinowska L, Palm S, Gibson K, Verbavatz JM, and Alberti S. 2015. Dictyostelium discoideum  
417 has a highly Q/N-rich proteome and shows an unusual resilience to protein aggregation.  
418 *Proc Natl Acad Sci U S A* 112:E2620-2629. 10.1073/pnas.1504459112
- 419 McGlinchey RP, Kryndushkin D, and Wickner RB. 2011. Suicidal [PSI+] is a lethal yeast prion.  
420 *Proc Natl Acad Sci U S A* 108:5337-5341.

- 421 Molina-Garcia L, Gasset-Rosa F, Alamo MM, de la Espina SM, and Giraldo R. 2018.  
422 Addressing Intracellular Amyloidosis in Bacteria with RepA-WH1, a Prion-Like Protein.  
423 *Methods Mol Biol* 1779:289-312. 10.1007/978-1-4939-7816-8\_18
- 424 Nakayashiki T, Kurtzman CP, Edskes HK, and Wickner RB. 2005. Yeast prions [URE3] and  
425 [PSI+] are diseases. *Proc Natl Acad Sci U S A* 102:10575-10580.
- 426 Necci M, Piovesan D, Dosztanyi Z, Tompa P, and Tosatto SCE. 2018. A comprehensive  
427 assessment of long intrinsic protein disorder from the DisProt database. *Bioinformatics*  
428 34:445-452. 10.1093/bioinformatics/btx590
- 429 Oldfield CJ, and Dunker AK. 2014. Intrinsically disordered proteins and intrinsically disordered  
430 protein regions. *Annu Rev Biochem* 83:553-584. 10.1146/annurev-biochem-072711-  
431 164947
- 432 Osherovich LZ, and Weissman JS. 2001. Multiple Gln/Asn-rich prion domains confer  
433 susceptibility to induction of the yeast [PSI(+)] prion. *Cell* 106:183-194. 10.1016/s0092-  
434 8674(01)00440-8
- 435 Pallares I, de Groot NS, Iglesias V, Sant'Anna R, Biosca A, Fernandez-Busquets X, and Ventura  
436 S. 2018. Discovering Putative Prion-Like Proteins in Plasmodium falciparum: A  
437 Computational and Experimental Analysis. *Front Microbiol* 9:1737.  
438 10.3389/fmicb.2018.01737
- 439 Pokrishevsky E, Grad LI, and Cashman NR. 2016. TDP-43 or FUS-induced misfolded human  
440 wild-type SOD1 can propagate intercellularly in a prion-like fashion. *Sci Rep* 6:22155.  
441 10.1038/srep22155

- 442 Ross ED, Maclea KS, Anderson C, and Ben-Hur A. 2013. A bioinformatics method for  
443 identifying Q/N-rich prion-like domains in proteins. *Methods Mol Biol* 1017:219-228.  
444 10.1007/978-1-62703-438-8\_16
- 445 Saupe SJ. 2011. The [Het-s] prion of *Podospora anserina* and its role in heterokaryon  
446 incompatibility. *Semin Cell Dev Biol* 22:460-468. 10.1016/j.semcdb.2011.02.019
- 447 Shahnawaz M, Park KW, Mukherjee A, Diaz-Espinoza R, and Soto C. 2017. Prion-like  
448 characteristics of the bacterial protein Microcin E492. *Sci Rep* 7:45720.  
449 10.1038/srep45720
- 450 Shen XX, Zhou X, Kominek J, Kurtzman CP, Hittinger CT, and Rokas A. 2016. Reconstructing  
451 the Backbone of the Saccharomycotina Yeast Phylogeny Using Genome-Scale Data. *G3*  
452 (*Bethesda*) 6:3927-3939. 10.1534/g3.116.034744
- 453 Shorter J, and Lindquist S. 2005. Prions as adaptive conduits of memory and inheritance. *Nat*  
454 *Rev Genets* 6:435-450.
- 455 Si K, Choi YB, White-Grindley E, Majumdar A, and Kandel ER. 2010. *Aplysia* CPEB can form  
456 prion-like multimers in sensory neurons that contribute to long-term facilitation. *Cell*  
457 140:421-435. 10.1016/j.cell.2010.01.008
- 458 Sideri T, Yashiroda Y, Ellis DA, Rodriguez-Lopez M, Yoshida M, Tuite MF, and Bahler J.  
459 2017. The copper transport-associated protein Ctr4 can form prion-like epigenetic  
460 determinants in *Schizosaccharomyces pombe*. *Microb Cell* 4:16-28.  
461 10.15698/mic2017.01.552
- 462 Su TY, and Harrison PM. 2019. Conservation of Prion-Like Composition and Sequence in Prion-  
463 Formers and Prion-Like Proteins of *Saccharomyces cerevisiae*. *Front Mol Biosci* 6:54.  
464 10.3389/fmolb.2019.00054

- 465 Sun Z, Diaz Z, Fang X, Hart MP, Chesi A, Shorter J, and Gitler AD. 2011. Molecular  
466 determinants and genetic modifiers of aggregation and toxicity for the ALS disease  
467 protein FUS/TLS. *PLoS Biol* 9:e1000614. 10.1371/journal.pbio.1000614
- 468 Tetz G, and Tetz V. 2017. Prion-Like Domains in Phagobiota. *Front Microbiol* 8:2239.  
469 10.3389/fmicb.2017.02239
- 470 Tetz G, and Tetz V. 2018. Prion-like Domains in Eukaryotic Viruses. *Sci Rep* 8:8931.  
471 10.1038/s41598-018-27256-w
- 472 True H, Berlin I, and Lindquist S. 2004. Epigenetic regulation of translation reveals hidden  
473 genetic variation to produce complex traits. *Nature* 431:184-187.
- 474 True H, and Lindquist S. 2000. A yeast prion provides a mechanism for genetic variation and  
475 phenotypic diversity. *Nature* 407:477-483.
- 476 Westaway D, Daude N, Wohlgemuth S, and Harrison P. 2011. The PrP-like proteins Shadoo and  
477 Doppel. *Top Curr Chem* 305:225-256. 10.1007/128\_2011\_190
- 478 Wickner R. 1994. [URE3] as an altered URE2 protein: evidence for a prion analog in  
479 *Saccharomyces cerevisiae*. *Science* 264:528-530.
- 480 Wickner R, Edskes H, Roberts B, Baxa U, Pierce M, Ross E, and Brachmann A. 2004. Prions:  
481 proteins as genes and infectious entities. *Genes Dev* 18:470-485.
- 482 Yuan AH, Garrity SJ, Nako E, and Hochschild A. 2014. Prion propagation can occur in a  
483 prokaryote and requires the ClpB chaperone. *Elife* 3:e02949. 10.7554/eLife.02949
- 484 Yuan AH, and Hochschild A. 2017. A bacterial global regulator forms a prion. *Science* 355:198-  
485 201. 10.1126/science.aai7776
- 486 Zambrano R, Conchillo-Sole O, Iglesias V, Illa R, Rousseau F, Schymkowitz J, Sabate R, Daura  
487 X, and Ventura S. 2015. PrionW: a server to identify proteins containing

488 glutamine/asparagine rich prion-like domains and their amyloid cores. *Nucleic Acids Res*  
489 43:W331-337. 10.1093/nar/gkv490  
490

# Figure 1

Correlation of various measures of mutational bias across proteomes versus the individual compositional bias in the Ure2p prion-forming domain, as judged by the fLPS program.

(a) Percentage of poly-N residues in the proteome. (b) Percentage of (poly-N + poly-Q) residues in the proteome. (c) DNA GC%. (d) Fraction of N/Q-rich prion-like proteins with fLPS P-value  $<1e-10$ . (e) Table of correlations and significances for plots (a) to (d).

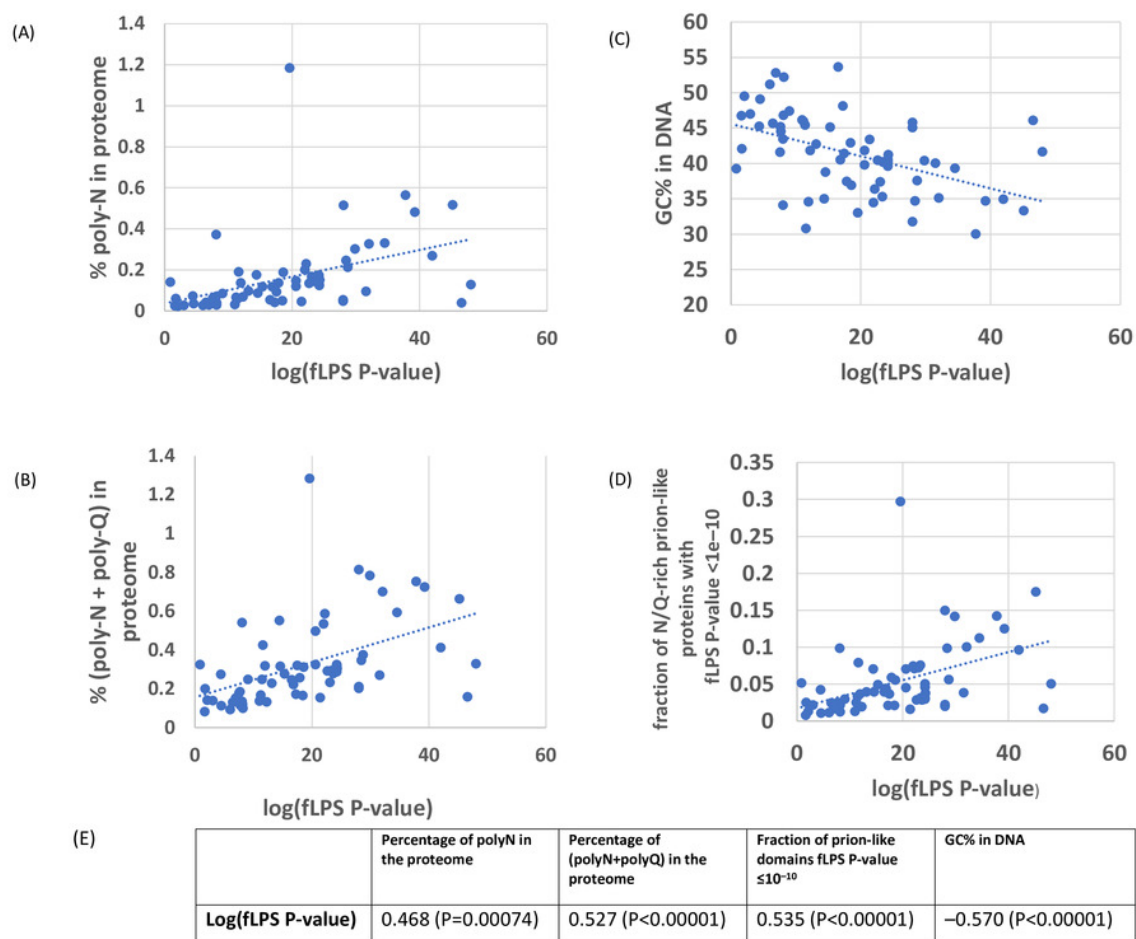
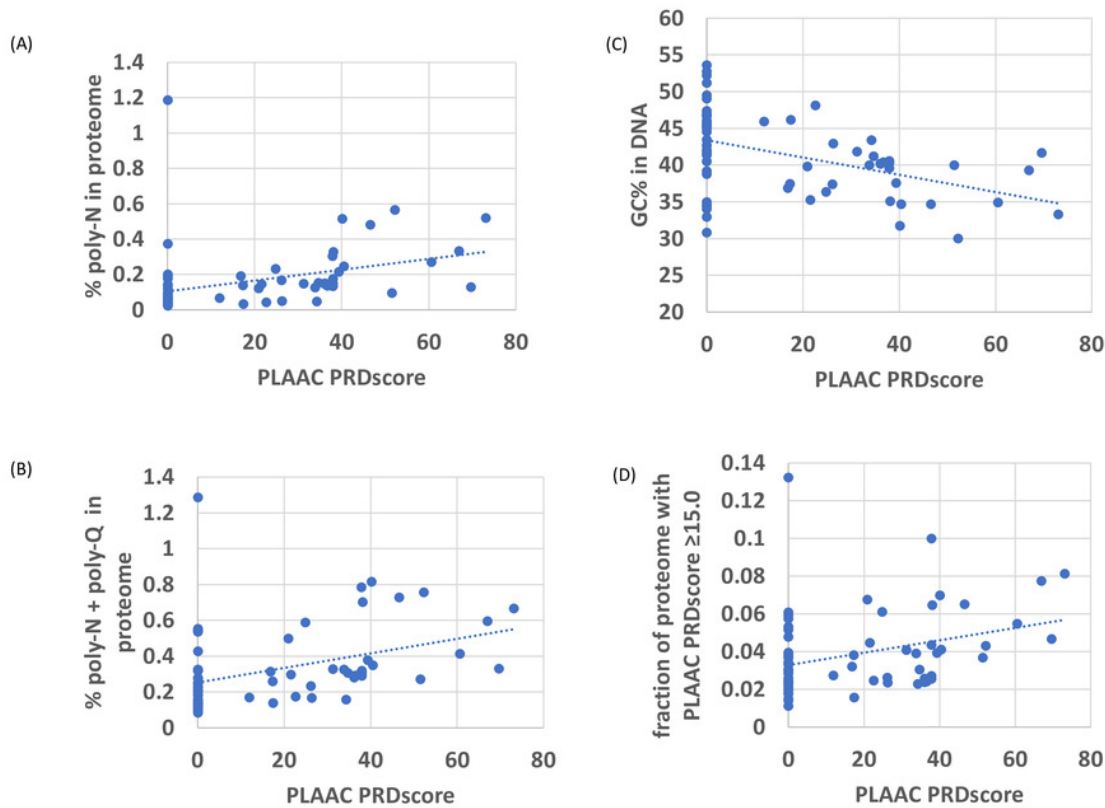


## Figure 2

As in Figure 1, except versus the individual PLAAC PRDscore in the Ure2p prion-forming domain.

(a) Percentage of poly-N residues in the proteome. (b) Percentage of (poly-N + poly-Q) residues in the proteome. (c) DNA GC%. (d) Fraction of proteome with PLAAC score  $\geq 15.0$ . (e) Table of correlations and significances for plots (a) to (d).



(E)

	Fraction of polyN in proteome	Fraction of (polyN+polyQ)	Fraction of prion-like domains fPLAAC PRD score $\geq 15.0$	GC% in DNA
<b>Log(fLPS P-value)</b>	0.388 (P=0.0013)	0.441 (P=0.00021)	0.424 (P=0.00039)	-0.539 (P<0.00001)

## Figure 3

Schematic evolutionary tree showing the distribution of orthologs with prion-like composition in different evolutionary families in the Uniprot reference set of fungal proteomes.

The organismal branching pattern from recent fungal phylogenies was used (Kurtzman & Robnett 2013; Shen et al. 2016) . The number of species in each family is given in brackets. The numbers of orthologs that are have fLPS P-value  $\leq 1e-10$  and PLAAC score  $\geq 15.0$  are listed in columns (Harrison 2017; Lancaster et al. 2014) .

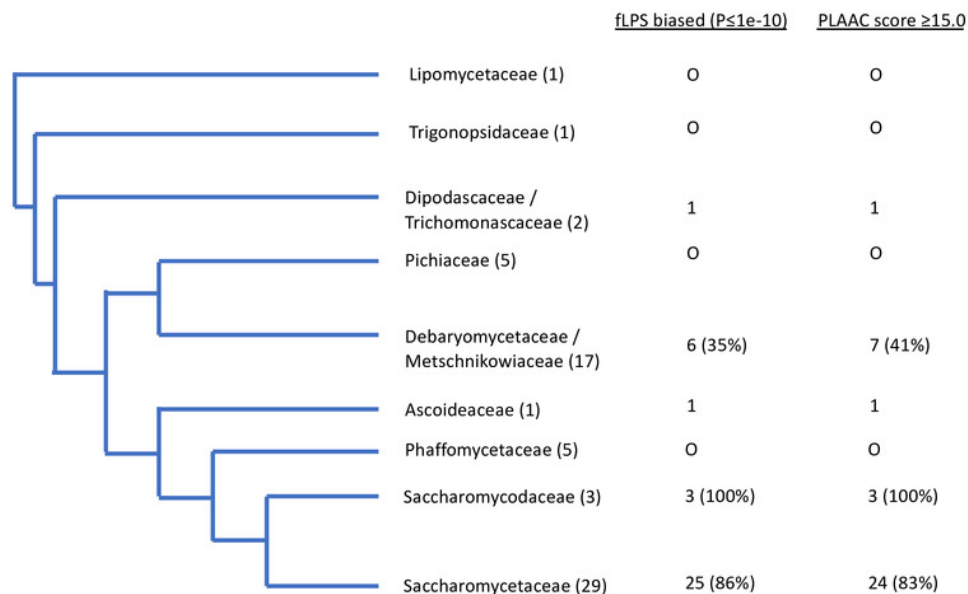


**Table 1** (on next page)

Coloured table for a set of known prion-forming domains of the correlations (weighted and un-weighted) between the compositional bias ( $-\log[\text{fLPS P-value}]$ ), and a variety of parameters.

Weighted correlations are the upper value in each cell, unweighted the lower value. Where removal of the common far outlier species *Ascoidea rubescens* causes increased significance for any correlation, the third and fourth rows in a cell display the correlation coefficients (in italics). For proteins which do not have an ortholog from *Ascoidea rubescens*, the name is labelled with '††'. If its removal causes no improvement in correlations, it is labelled with '†'. Correlations significant at  $\leq 0.0005$  are labelled \*\*\* and coloured green, significant at  $> 0.0005$  and  $\leq 0.0016$  labelled \*\* and coloured orange, and  $> 0.0016$ , and  $\leq 0.05$  are labelled \*). The threshold 0.0016 comes from a Bonferroni correction to allow for the fact that 31 sequences are being tested for a correlation against any specific proteome-wide property. In column one, the name is colour-coded according to the most significant correlation, with underlining if it is a 1-\* correlation.

Protein (Number of orthologs in brackets)	%N in proteome	%Q in proteome	%poly-N	%poly-Q	%poly- Q+%poly-N	DNA GC%	Fraction of N/Q-rich proteins in the proteome by fLPS bias threshold		
							Threshold 1e-08	Threshold 1e-10	Threshold 1e-12
<b>Known amyloid-based prions in <i>S. cerevisiae</i></b>									
<b>Sup35</b> <b>P05453 (62)</b>	0.237	0.042	0.132	0.415 **	0.278 *	-0.351 *	0.218	0.202	0.187
	0.136	0.060	0.035	0.380 *	0.180	-0.263 *	0.142	0.119	0.095
	0.350 *	0.019	0.315 *	0.411 **	0.409 **	-0.388 *	0.348 *	0.353 *	0.366 *
	0.316 *	0.021	0.307 *	0.370 *	0.385 *	-0.323 *	0.348 *	0.356 *	0.368 *
<b>Swi1 ††</b> <b>P09547 (56)</b>	0.661 ***	-0.149	0.603 ***	0.074	0.544 ***	-0.498 ***	0.643 ***	0.627 ***	0.607 ***
	0.628 ***	-0.184	0.570 ***	0.016	0.473 ***	-0.510 ***	0.600 ***	0.586 ***	0.568 ***
<b>Cyc8</b> <b>P14922 (61)</b>	0.387 *	0.292 *	0.320 *	0.361 *	0.409 **	-0.472 ***	0.398 **	0.385 *	0.364 *
	0.251	0.320 *	0.165	0.305 *	0.254 *	-0.305 *	0.240	0.234	0.225
	0.522 ***	0.278 *	0.577 ***	0.354 *	0.567 ***	-0.507 ***	0.563 ***	0.581 ***	0.595 ***
	0.368 *	0.307 *	0.350 *	0.297 *	0.382 *	-0.334 *	0.374 *	0.394 *	0.418 **
<b>Ure2</b> <b>P23202 (66)</b>	0.571 ***	0.241	0.468 ***	0.357 *	0.527 ***	-0.570 ***	0.556 ***	0.535 ***	0.495 ***
	0.485 ***	0.253 *	0.420 ***	0.330 *	0.476 ***	-0.478 ***	0.470 ***	0.453 ***	0.423 ***
	0.682 ***	0.246 *	0.676 ***	0.361 *	0.651 ***	-0.584 ***	0.687 ***	0.696 ***	0.690 ***
	0.566 ***	0.259 *	0.590 ***	0.332 *	0.563 ***	-0.484 ***	0.568 ***	0.576 ***	0.572 ***
<b>Rnq1 †</b> <b>P25367 (26)</b>	0.139	-0.381	0.096	-0.193	0.037	-0.080	0.081	0.053	0.010
	0.230	-0.431 *	0.159	-0.197	0.090	-0.159	0.070	0.040	0.001
<b>Mot3 †</b> <b>P54785 (25)</b>	0.460 *	-0.420 *	0.395	0.371	0.439 *	-0.468 *	0.385	0.386	0.399 *
	0.393	-0.507 *	0.264	0.268	0.299	-0.409 *	0.140	0.129	0.146
<b>Nu100 †</b> <b>Q02629 (11)</b>	0.154	0.107	-0.110	-0.105	-0.518	-0.008	-0.012	-0.027	-0.047
	0.224	0.148	-0.058	0.013	-0.499	-0.090	-0.017	-0.030	-0.042
<b>Pin3 †</b> <b>Q06449 (55)</b>	0.198	0.022	0.230	0.000	-0.121	-0.183	0.209	0.198	0.179
	0.179	-0.030	0.200	-0.014	-0.046	-0.169	0.165	0.153	0.137
<b>Other prion-forming domains discussed in the text</b>									
<b>New1 ††</b> <b>Q08972 (63)</b>	0.566 ***	0.269 *	0.476 ***	0.191	0.482 ***	-0.482 ***	0.513 ***	0.501 ***	0.486 ***
	0.521 ***	0.261 *	0.442 ***	0.188	0.439 ***	-0.449 ***	0.468 ***	0.458 ***	0.446 ***
<b>Pub1</b> <b>P32588 (62)</b>	0.469 ***	0.365 *	0.484 ***	0.707 ***	0.686 ***	-0.547 ***	0.545 ***	0.545 ***	0.533 ***
	0.457 ***	0.243	0.426 **	0.620 ***	0.597 ***	-0.532 ***	0.449 ***	0.448 ***	0.442 ***
	0.466 ***	0.401 **	0.551 ***	0.734 ***	0.728 ***	-0.534 ***	0.567 ***	0.584 ***	0.594 ***
	0.450 ***	0.278 *	0.459 ***	0.646 ***	0.622 ***	-0.518 ***	0.447 ***	0.459 ***	0.471 ***

**Table 2** (on next page)

Coloured table for a set of known prion-forming domains of the correlations (both weighted and un-weighted) between the prion-like composition (PLAAC PRDscore) and a variety of parameters.

Weighted correlations are the upper value in each cell, unweighted the lower value. Where removal of the common far outlier species *Ascoidea rubescens* causes increased significance for any correlation, the third and fourth rows in a cell display the correlation coefficients (in italics). For proteins which do not have an ortholog from *Ascoidea rubescens*, the name is labelled with '††'. If its removal causes no improvement in correlations, it is labelled with '†'. Correlations significant at  $\leq 0.0005$  are labelled \*\*\* and coloured green, significant at  $> 0.0005$  and  $\leq 0.0016$  labelled \*\* and coloured orange, and  $> 0.0016$ , and  $\leq 0.05$  are labelled \*). The threshold 0.0016 comes from a Bonferroni correction to allow for the fact that 31 sequences are being tested for a correlation against any specific proteome-wide property. In column one, the name is colour-coded according to the most significant correlation, with underlining if it is a 1-\* correlation.

Protein (Number of orthologs in brackets)	%N in proteome	%Q in proteome	%poly-N	%poly-Q	%poly- Q+%poly- N	DNA GC%	Fraction of prion-like proteins in the proteome by PLAAC PRDscore		
							≥0.0	≥15.0	≥30.0
<b>Known amyloid-based prions in <i>S. cerevisiae</i></b>									
<b>Sup35</b> <b>P05453 (62)</b>	0.292 * 0.160 <i>0.457 ***</i> <i>0.407 **</i>	0.268 * 0.254 * <i>0.245</i> <i>0.215</i>	0.174 0.040 <i>0.437 ***</i> <i>0.411 **</i>	<i>0.423 **</i> 0.372 * <i>0.421 **</i> <i>0.363 *</i>	0.313 * 0.181 <i>0.497 ***</i> <i>0.454 ***</i>	-0.345 * -0.252 * <i>-0.401 **</i> <i>-0.336 *</i>	<i>0.429 ***</i> 0.307 * <i>0.574 ***</i> <i>0.528 ***</i>	0.369 * 0.224 <i>0.560 ***</i> <i>0.506 ***</i>	0.273 * 0.108 <i>0.525 ***</i> <i>0.461 ***</i>
<b>Swi1 ††</b> <b>P09547 (56)</b>	<i>0.475 ***</i> <i>0.465 ***</i>	-0.206 -0.200	<i>0.451 ***</i> <i>0.431 **</i>	0.074 0.054	<i>0.414 **</i> 0.375 *	<i>-0.471 ***</i> <i>-0.470 ***</i>	<i>0.460 ***</i> <i>0.443 **</i>	<i>0.464 ***</i> <i>0.441 **</i>	<i>0.442 **</i> 0.411 *
<b>Cyc8</b> <b>P14922 (61)</b>	0.353 * 0.244 <i>0.453 ***</i> <i>0.328 *</i>	0.250 0.285 * <i>0.242</i> <i>0.279 *</i>	0.325 * 0.183 <i>0.535 ***</i> <i>0.324 *</i>	<i>0.421 **</i> 0.356 * <i>0.417 **</i> <i>0.353 *</i>	<i>0.438 ***</i> 0.288 * <i>0.569 ***</i> <i>0.389 *</i>	<i>-0.458 ***</i> -0.301 * <i>-0.482 ***</i> <i>-0.319 *</i>	<i>0.563 ***</i> <i>0.462 ***</i> <i>0.645 ***</i> <i>0.544 ***</i>	<i>0.486 ***</i> 0.385 * <i>0.608 ***</i> <i>0.503 ***</i>	0.375 * 0.274 * <i>0.548 ***</i> <i>0.429 **</i>
<b>Ure2</b> <b>P23202 (66)</b>	<i>0.495 ***</i> <i>0.448 ***</i> <i>0.683 ***</i> <i>0.594 ***</i>	0.151 0.087 <i>0.130</i> <i>0.071</i>	<i>0.388 **</i> 0.369 * <i>0.704 ***</i> <i>0.631 ***</i>	0.308 * 0.246 * <i>0.297 *</i> <i>0.239</i>	<i>0.441 ***</i> <i>0.401 **</i> <i>0.645 ***</i> <i>0.548 ***</i>	<i>-0.539 ***</i> <i>-0.453 ***</i> <i>-0.586 ***</i> <i>-0.483 ***</i>	<i>0.494 ***</i> <i>0.388 **</i> <i>0.627 ***</i> <i>0.484 ***</i>	<i>0.424 ***</i> 0.333 * <i>0.615 ***</i> <i>0.465 ***</i>	0.314 * 0.226 <i>0.567 ***</i> <i>0.393 **</i>
<b>Rnq1 †</b> <b>P25367 (26)</b>	-0.001 0.079	-0.264 -0.340	-0.046 0.005	-0.267 -0.242	-0.107 -0.058	0.035 -0.027	-0.128 -0.137	-0.128 -0.139	-0.133 -0.199
<b>Mot3 †</b> <b>P54785 (25)</b>	0.149 0.153	-0.166 -0.336	0.135 0.057	0.314 0.213	0.196 0.103	-0.159 -0.172	0.114 -0.107	0.212 -0.014	0.283 -0.046
<b>Nu100 †</b> <b>Q02629 (11)</b>	0.090 0.169	0.283 0.303	-0.185 -0.122	-0.030 0.075	-0.165 -0.083	-0.003 -0.084	0.304 0.290	0.142 0.160	0.021 -0.024
<b>Pin3 †</b> <b>Q06449 (55)</b>	0.000 -0.010	0.282 * 0.226	0.025 0.005	0.222 0.202	0.121 0.100	-0.081 -0.067	0.112 0.006	0.113 0.029	0.159 0.056
<b>Other prion-forming domains discussed in the text</b>									
<b>New1 ††</b> <b>Q08972 (63)</b>	0.368 * 0.339 *	0.236 0.250 *	0.301 * 0.288 *	0.183 0.226	0.326 * 0.327 *	-0.369 * -0.368 *	0.412 * 0.419 *	0.377 * 0.380 *	0.299 * 0.291 *
<b>Pub1</b> <b>P32588 (62)</b>	0.226 0.241 <i>0.232</i> <i>0.247</i>	<i>0.521 ***</i> <i>0.424 **</i> <i>0.540 ***</i> <i>0.443 ***</i>	0.300 * 0.255 * <i>0.381 *</i> <i>0.290 *</i>	<i>0.756 ***</i> <i>0.679 ***</i> <i>0.771 ***</i> <i>0.703 ***</i>	<i>0.559 ***</i> <i>0.479 ***</i> <i>0.628 ***</i> <i>0.535 ***</i>	-0.279 * -0.309 * <i>-0.274 *</i> <i>-0.303 *</i>	<i>0.597 ***</i> <i>0.504 ***</i> <i>0.631 ***</i> <i>0.532 ***</i>	<i>0.605 ***</i> <i>0.509 ***</i> <i>0.674 ***</i> <i>0.570 ***</i>	<i>0.570 ***</i> <i>0.465 ***</i> <i>0.695 ***</i> <i>0.571 ***</i>

## Figure 4

Correlations of %K (lysine residues) within the N/Q-rich regions of prion-forming proteins plotted versus the overall %K trend in proteomes.

Blue points are for the set of known amyloid-based prions in Figure 4, and orange points for the total list of prion-forming domains including those listed in Table S2.

